

The NN Phase Shifts < 3 GeV and Resonance Features ^{*}

Funk, A. and von Geramb, H.V.

*Theoretische Kernphysik, Universität Hamburg,
Luruper Chaussee 149, D-22761 Hamburg, Germany*

Abstract

Solutions SP00, SM00 and FA00 of nucleon-nucleon (NN) phase shift analyzes by Arndt *et al.* are used in optical model studies. The partial waves, single channels $J \leq 7$ and coupled channels $J \leq 6$, are scrutinized. The radial probability distributions and losses of flux are used to identify the known Δ and N^* resonances as well as anticipated other structures. The energy interval extends to 3 GeV.

^{*} To appear in the Proceedings of the International Workshop on Resonances in Few-Body Systems, 4-8 September 2000, Sarospatak Hungary, Few-Body Systems, Supplement, Springer Verlag

I. INTRODUCTION AND SALIENT FEATURES

In view of an optical model study it is timely to review the current situation of nucleon-nucleon phase shift data below 3 GeV [1]. NN scattering is a long standing problem for more than five decades and has been reviewed under many different aspects, this in progress as the data base developed, see Fig. 1. We use as derived quantities the *phase shifts*,

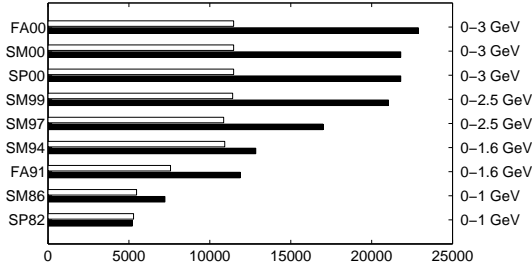


FIG. 1: History of database SAID 1980-2000, solid bars are pp data and open bars are np data

taken exclusively from SAID[1]. The low energy data, < 400 MeV, received particular attention by Arndt *et al.*, see solutions in Fig. 2, and the Nijmegen group in their NN elastic scattering analysis below $T_\ell \leq 350$ MeV[2]. Above pion threshold, ~ 280 MeV, reaction channels open in a way shown in Fig. 3. The low energy data, < 300 MeV,

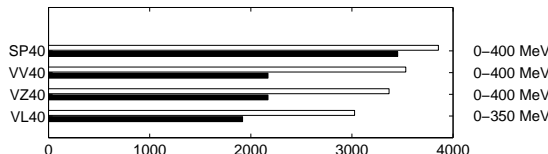


FIG. 2: The same as shown in Fig. 1 but restricted to sub-threshold data

are subject of NN potentials which we use as reference potentials. The classical meson exchange potentials from Nijmegen, Paris, Bonn, and our recent OSBEP [3] potential fit the on-shell data within a few percent. They differ little in their near off-shell t-matrices. The Gel'fand-Levitman-Marchenko integral equations relate directly phase shifts with off-shell t-matrices. For convenience this link is parameterized in terms of inversion potentials and the Lippmann-Schwinger equation[4, 5]. In Fig. 4 is shown a sample of potentials which reproduce the low energy phase shifts. They allow to distinguish a long range Yukawa tail, a medium range attraction $\sim 1 - 2$ fm and a short range repulsion. From these potentials,

equally valid for the boson exchange potentials, we draw the conclusion that the long and medium range NN interaction diminish in their importance for energies above 500 MeV. For projectiles with $T_\ell > 1$ GeV the repulsive core is remaining and predominantly causes scattering. The core strength reaches a value of 1 GeV at ~ 0.5 fm which may be viewed as the classical turning point.

The real new feature above 300 MeV is the occurrence of inelasticity and thus breakdown of unitarity of the elastic channel S-matrix. However, the above mentioned potentials may still be compared with the real parts of phase shifts. From the theoretical contents of boson exchange models and their similar parameterization it is expected that they extrapolate from the fitted domain < 300 MeV towards higher energies with the same closeness as in the fitted domain. As is shown in Figs. 5 and 6 this is not the case. We argue that off-shell differences in the high quality potentials are essentially caused by these high energy differences, made visible in the on-shell data $0.3 - 3$ GeV.

The actual phase shifts cover the energy range up to 3 GeV for pp scattering and 1.2 GeV for np scattering. This is ten times more than what the classical potentials describe. Their extrapolation towards higher energies is quite different for each solution and by dint of its construction only inversion potentials follow closely the real part of the phase shifts at all energies.

II. OPTICAL MODEL ANALYSIS

The loss of unitarity is met by an optical model potential. Such potential approaches are well known from nucleon-nucleus scattering and are used for NN scattering as well[6, 7, 8]. In

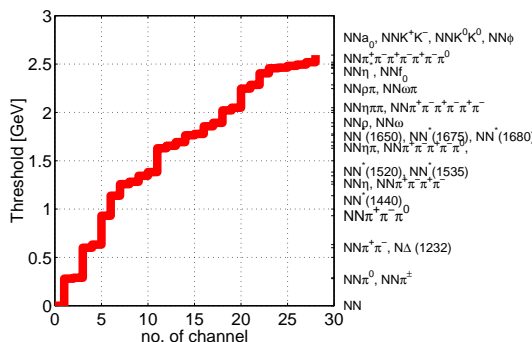


FIG. 3: NN induced reaction channels

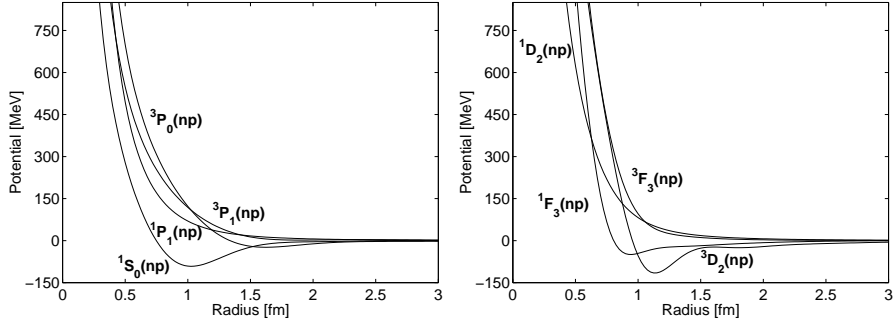


FIG. 4: Nucleon-nucleon inversion potentials using SP00 phases

another contribution to these proceedings, where the theoretical and technical background of the optical model was introduced, we distinguish real reference potentials and complex valued separable potentials (or complex boundary conditions instead). This model is used together with an appraisal of the data shown next. In Figs. 5 and 6 the SM97 and FA00 solutions are shown together with potential model phase shifts, $J \leq 3$, Nij-1, AV18, HH-inv. Arndt's solutions SM97 and FA00 are stable. Further on, we shall use the solution FA00 (it differs from SP00 and SM00 only marginally). In Fig. 8 we show the results of optical model calculations in which the reference potentials are Gel'fand-Levitan-Marchenko potentials with a rank one separable potential (harmonic oscillators $\phi_\ell(r, \hbar\omega = 450\text{MeV})$). The reference potential phase shifts are shown together (as dotted lines) with the real phase shift data (continuous solution) and radial distributions of probabilities and loss of flux.

$$\rho(r, \alpha, E) = \text{Trace } \Psi^\dagger(r, \alpha, E) \Psi(r, \alpha, E) r^{-2} \quad (1)$$

and the loss of flux, from the continuity equation

$$\frac{\partial}{\partial t} \rho(r) + (\vec{\nabla} \cdot \vec{j}) = 0, \quad (2)$$

$$(\vec{\nabla} \cdot \vec{j}) := \text{Trace } \frac{i}{\hbar} < \Psi(\alpha, E) | \mathcal{V}(., r) - \mathcal{V}^\dagger(r, .) | \Psi(\alpha, E) >. \quad (3)$$

A glance upon reaction and inelastic channels is useful. In Fig. 3 are channels plotted against threshold energy. The region 0.5-1 GeV is dominated by the $\Delta(1232)$ resonance whereas several N^* resonances shape the region 1-2 GeV[9]. In the high energy region, ~ 2.5 GeV, we see many production channels opening. These reactions couple within several partial waves so the effects are smoothly distributed and we have good conditions for an analysis with a smooth optical potential.

A mental image of the reaction sequence is shown in Fig. 7. First, the two nuclei approach each other and their respective meson clouds are exerting the boson exchange forces upon each other. The nuclei are still well separated (long and medium range forces). Next, after further approach, one or both nucleons are intrinsically excited into intermediate states which rapidly de-excite by particle emission. The scattering may be either elastic or inelastic into three and more body systems. The image suggests no fusion of the two nucleons, which is a feature quite different from the studied πN resonance formation. The Pauli principle is very effective in generating the repulsive core and it appears also effective in the conservation of individual nucleons. At $T_\ell = 2 - 3$ GeV they are well separated in momentum space.

III. PROBABILITY AND LOSS OF FLUX

In Fig. 8 we show as a function of radius and energy the probability density and the loss of flux. Four diagrams, arranged in a 2×2 matrix, belong to one channel. Diagram-11 contains the real δ_α (solid line for continuous solution and crosses for single energy solutions), and the inversion potential, see Fig. 4, reference phases (shaded), diagram-12 contains the absorption angle ρ_α (the reference potential generates no absorption), diagram-21 shows probability surfaces as a function of energy and radius, diagram-22 shows surfaces of loss of flux as a function of energy and radius. For coupled channels we show in Fig. 8 the traces of probabilities and currents for the 3SD_1 and 3PF_2 channels. For the $T = 0$ channels only np data, < 1.2 GeV, contribute and Arndt's solution > 1.2 GeV is not determined from data. This becomes relevant in 1P_1 , 3SD_1 . The figures support the mental image claimed above in which nucleons do not fuse and their individuality is maintained. The produced mesons stem from one or the other nucleon and not from a fused compound system. The strengths of separable potentials yield large tables, are available on request, and shall be published elsewhere. They show the Δ resonance and N^* contributions in the relevant partial waves with the implication that all dependencies are very smooth over many hundreds of MeV. None of the results support the formation of intermediate fused NN systems, at least the phase shift solutions do not support any such formation.

IV. SUMMARY

The primary purpose of this study was a comparison of the Paris, Nij-2, Reid93, AV18, Nij-1, ESC96 and inversion potentials in the realm of an optical model extension using boundary conditions and/or separable potentials. Applications are in progress for studies of microscopic nucleon-nucleus scattering analysis in folding models, studies of exotic nuclei and calculations needed in the technology of waste management with medium energy particles. Despite these classical applications we seek collaboration with groups pursuing QCD inspired theoretical development and calculations.

- [1] R.A. Arndt *et al.*: SAID via *telnet*: said.phys.vt.edu, *user*: said (no password)
- [2] V.G.J. Stoks, R.A.M. Klomp, M.C.M. Rentmeester, and J.J. de Swart: Phys. Rev. **C48**, 792 (1993)
- [3] L. Jaede: Phys. Rev. **C58**, 96 (1998)
- [4] Th. Kirst: J. Math. Phys. **32**, 1318 (1991)
- [5] M. Sander and H.V. von Geramb: Springer, Lecture Notes in Physics **488**, 141 (1997)
- [6] V.G. Neudatchin, N.P. Yudin, Y.L. Dorodnykh, and I.T. Obukhovsky: Phys. Rev. **C43**, 2499 (1991)
- [7] H.V. von Geramb, K.A. Amos, H. Labes, and M. Sander: Phys. Rev. **C58**, 1948 (1998)
- [8] A. Faltenbacher: Diplomarbeit, Hamburg (1999)
- [9] D.E. Groom *et al.*, (Particle Data Group): Eur. Phys. Jour. **C15**, 1 (2000)(URL: <http://pdg.lbl.gov>)

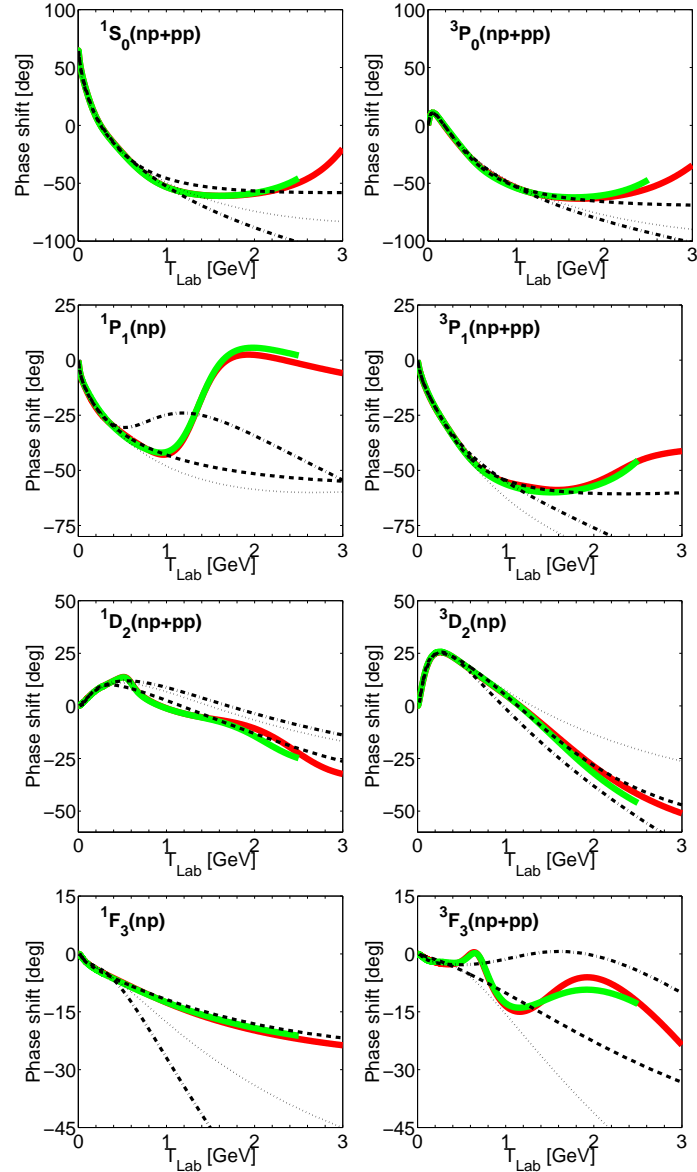


FIG. 5: SM97 (shaded, < 2.5 GeV) and FA00 (shaded, < 3 GeV) phase shifts and reference phase shifts from HH-inv (dashed), Nij-1 (dash-dotted) and AV18 (dotted)

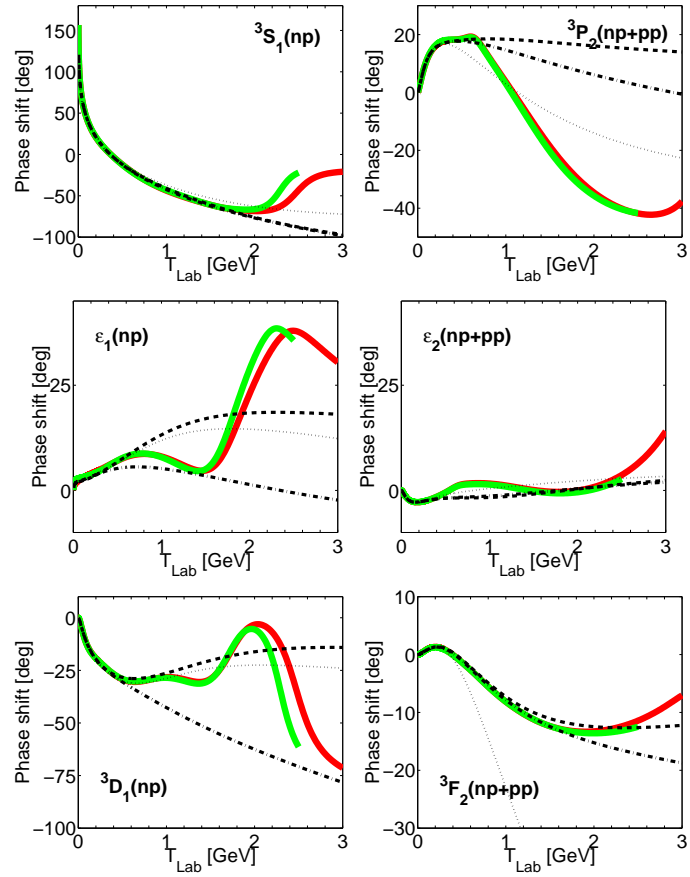


FIG. 6: As previous figure but for the coupled channels 3SD_1 and 3PF_2

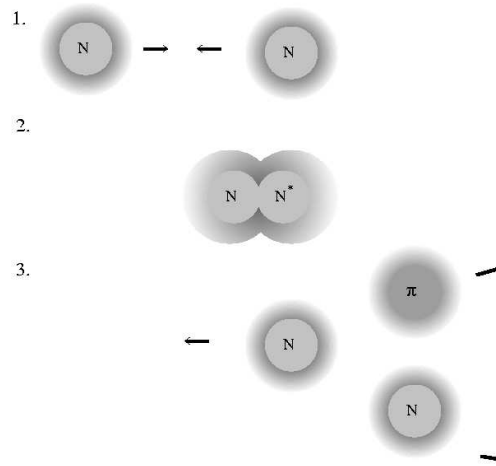


FIG. 7: Guide to mental image of NN interaction sequence

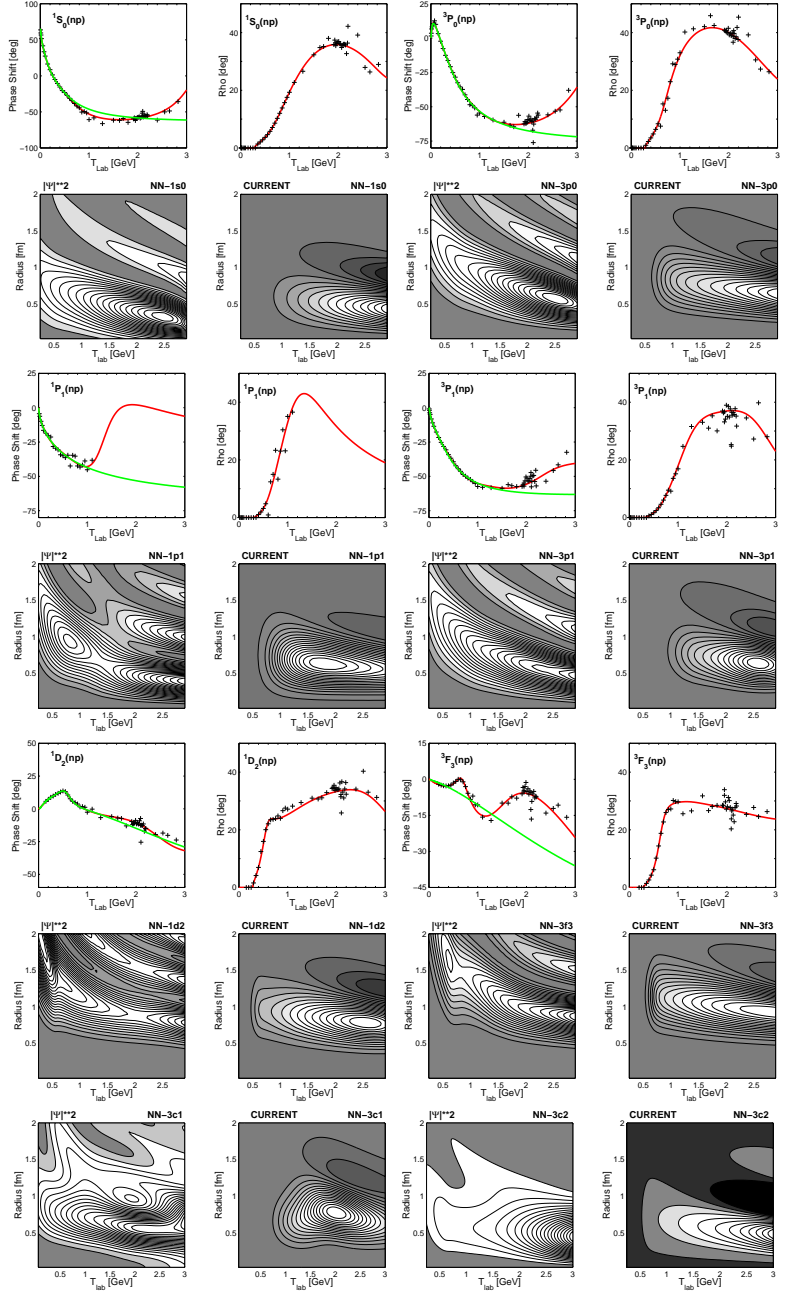


FIG. 8: Block matrices containing the reproduced δ and ρ of FA00 and energy/radial probabilities with loss of flux